SoC Estimation of Lithium Battery Based on Fully Connected Deep Neural Network

Zhenkai Qin[1], Mingfu Zhu[2], Yizhe Zhang[2], Shangxin Liu[3], Yawei Chen[3]

[1]School of Physics, Engineering and Technology, University of York, York YO10 5DD, UK
[2]School of Computer Science and Technology, Henan Polytechnic University, Jiaozuo 454003, China

[3]Henan Chuitian Technology Co., Ltd., Hebi 458030, China

Abstract

In order to improve the estimation accuracy of the State of Charge (SoC) of lithium batteries, in view of the nonlinear mapping characteristics of battery data and the inadequacy of shallow neural network mapping, lithium iron phosphate batteries were taken as the research object, TensorFlow and Keras as the support of the experimental platform, and a Fully Connected Deep Neural Network (FCDNN) was proposed to establish the SOC prediction model for lithium batteries. Experimental data were obtained from the Center for Advanced Life Cycle Engineering (CALCE) at the university of Maryland. With current, voltage and resistance as the main inputs of the model, and SOC as the output, the training set was used to train the FCDNN model, and the verification set was used for verification. The training set and the verification set were divided by the 4-fold cross validation method, and the performance of the model was verified while the FCDNN model was trained. Finally, the test set is used to test the resulting model. The results show that the mean absolute error (MAE) of SOC prediction using FCDNN model is 0.954%, the model estimation error is kept within 3%, and the estimated time for a single sample is 5ms. The validity of FCDNN was verified by comparing the prediction errors of FCDNN with different hidden layers, traditional Back Propagation Neural Network (BPNN) and Ampere-hour integral method.

Keywords

State of Charge; Fully Connected Deep Neural Network; Lithium Iron Phosphate Battery; 4-Fold Cross Validation Method; TensorFlow; Keras.

1. INTRODUCTION

In recent years, with the aggravation of environmental pollution, more and more people begin to realize the seriousness of environmental pollution. Use of renewable clean energy will relieve the pressure on environment pollution. As the carrier of clean energy, battery has become the research object of domestic and foreign scholars. Lithium iron phosphate battery has the advantages of low cost, high energy, long service life, environmental protection and so on, and gradually become the mainstream of the development of power battery[1]. In addition, the perfect battery management system (BMS) will always monitor the battery status, in order to extend the battery life. The BMS has many functions such as State of Health (SoH) estimation and State of Charge (SoC) estimation[2]. Battery SoC cannot be measured directly but must be inferred from observed variables, such as current and voltage[3]. Due to the nonlinear nature of the battery, the SoC of the battery is difficult to estimate[4].

ISSN: 2472-3703 DOI: 10.6911/WSRJ.202502_11(2).0002

The current SoC estimation methods include ampere-hour integral method, Open Circuit Voltage (OCV), kalman filter method, neural network method, etc. The Ampere-Hour integral method estimates battery SoC through accumulating battery current over time directly[5]. This method will gradually produce cumulative error, and need to know in advance the initial SoC value of the system. The OCV method is usually employed to calibrate the SoC value through a look-up table between SoCs and OCVs, but it is not applicable for batteries with a flat voltage plateau, which would result in considerable estimation errors[6]. Kalman filtering algorithm is often tied to some battery model, like a lumped parameter model or an equivalent circuit model which require arduous model identification to adequately represent the non-linear behavior of battery[7]. The large computational burden is usually an obstacle for feasible implementation of such methods; it also reflects on the cost of the BMS and the whole system [8]. Artificial Neural Network (ANN) is well suited for modelling complex and time-varying systems. It will not depend on battery model and mathematical relationship. ANN is very suitable for modeling complex time-varying systems, independent of battery models and mathematical relationships [9]. By choosing the appropriate training algorithm, activation function, hidden layer number, neuron number, learning rate, extension value, input and output order, the computational complexity of neural network can be reduced [10]. SoC estimation methods for neural networks mainly include Back-Propagation Neural Networks (BPNN)[11][12], Recurrent Neural Networks (RNN)[13][14]. The existing artificial neural network cannot map the external property value of lithium battery to the target value SoC more accurately.

In recent years, the neural network based deep learning method has drawn much attention from the research world[15]. The TensorFlow[16], a deep learning framework, provides the ability to quickly prototype and test different network architectures, automatically calculating the results of back propagation.

Aiming at the accurate estimation of SoC in battery management system and the insufficient mapping of shallow neural network. The data set for the K2 lithium iron phosphate battery was measured by the battery research group at the Center for Advanced Life Cycle Engineering (CALCE)[17] at the university of Maryland. A Fully Connected Deep Neural Network (FCDNN) is proposed to predict the SoC of lithium batteries. The experiment is based on Jupyter Notebook and TensorFlow and Keras. The prediction results of FCDNN with different hidden layers, BPNN and Ann hour integration method were compared. The training set and verification set were divided by the 4-fold cross validation method, and the test set was set aside separately. The Adam optimization algorithm in the deep learning framework was used to replace the traditional stochastic gradient descent algorithm. The FCDNN has stronger nonlinear mapping ability than the shallow BPNN.

2. FCDNN MODEL

Traditional machine learning techniques contain no more than one or two layers of non-linear and linear transformations[18]. The deep neural network enables the neural network to compactly represent the highly nonlinear complex mapping of large training data sets[19]. The structure of L-layer deep neural network is composed of input layer, hidden layer and output layer. The input layer inputs the attribute value, and the output layer outputs the prediction target value. Architecture of deep neural network as shown in Fig.1.;

ISSN: 2472-3703 DOI: 10.6911/WSRJ.202502_11(2).0002

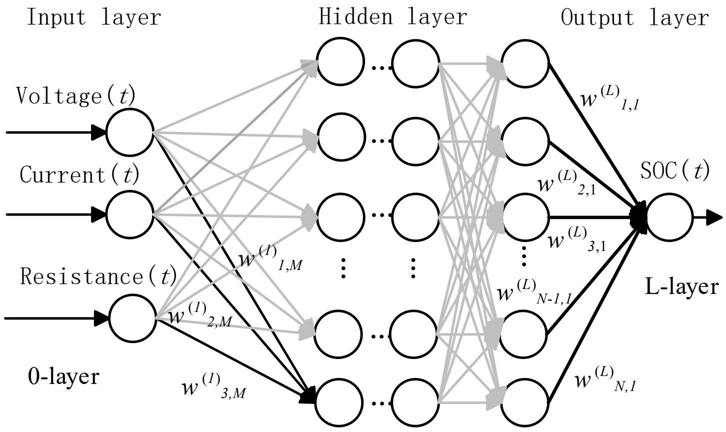

Figure 1. Architecture of deep neural network

In the Fig.1: t represents the time step t; $W^{(L)}N,M$ represents the weight between node N in layer $L-1$ and node M in layer L. N and M can be equal.

The calculation time of the depth neural network model is exponentially increased with the number of hidden layer nodes, and the direct proportional function of hidden layer is increased [7]. It can be seen that adding more hidden layers will not increase the calculation time of the model rapidly, and the input value can be more accurately mapped to the target value SoC. As a result, FCDNN of different depths is constructed, the input layer is Voltage, Current and Resistance, and the output layer is SoC. FCDNN model hiding layer sets 10 nodes in each layer. FCDNN models with 4, 8 and 12 layers were constructed respectively.

Flowchart FCDNN model as show in Fig.2.

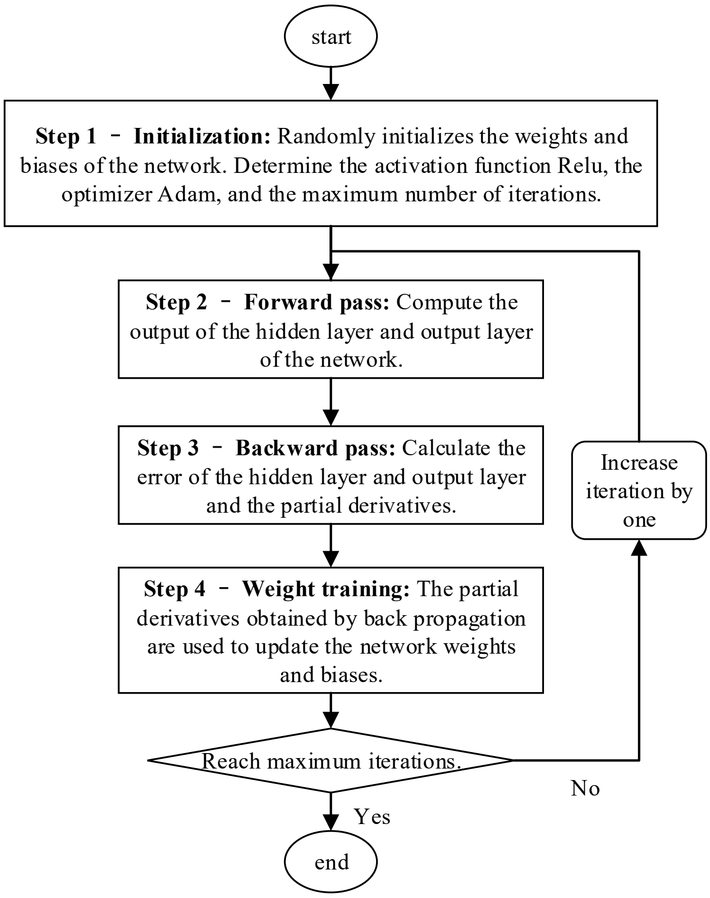

Figure 2. Flowchart FCDNN model

ISSN: 2472-3703 DOI: 10.6911/WSRJ.202502_11(2).0002

Step 1: FCDNN model was established and model parameters were randomly weights and biases.

Step 2: Forward propagation of the network begins when the training data set is entered into the network and the SoC estimate for each time step is calculated and the total loss function is determined. Define the following variables: l is equal to L; t represents the time step t; $a^{(l)}n$ represents the output value of node n in l layer; $a^{(l-1)}j$ represents the output value of layer j of $l-1$; $w^{(l)}j,n$ and $b^{(l)}j,n$ respectively represent the weight and bias between the node n of layer l and the node j of layer $l-1$.

$$a_n^{(l)}(t) = f(\sum_j (w_{j,n}^{(l)} * a_j^{(l-1)}(t) + b_{j,n}^{(l)})) \tag{1}$$

$$SoC(t) = a_n^{(l)}(t) \tag{2}$$

SoC(t) is the estimated SoC at the time step t calculated by the network. In order to make the model and realize the nonlinear transformation, used in the network of hidden layer nodes Rectified Liner Units (Relu) activation function;

$$f = \max(0,\ a) \tag{3}$$

Step 3: Every iteration of the neural network in the training process, its output layer will produce an error signal, that is, the difference between the estimated value of the model SoC and the actual value. Mean Square Error (MSE) is set as the model loss function.

$$MSE(\mathbf{X},\mathbf{Y}) = \frac{1}{m}\sum_{i=1}^{m}(h(x(i)) - y(i))^2 \tag{4}$$

Where m represents the number of samples. ***X*** and ***Y*** represent the attribute value and SoC real value of the sample data set respectively. $h()$ function represents the FCDNN model that has been trained. $h(x(i))$ represents the SOC estimate of the model for sample i, that is, $x(i)$; $y(i)$ represents the real value of SoC. In order to observe when the model reached the optimal state in the training process, the Mean Absolute Error (MAE) in all iteration steps was output.

$$MAE(\mathbf{X},\mathbf{Y}) = \frac{1}{m}\sum_{i=1}^{m}\left|h(x(i)) - y(i)\right| \tag{5}$$

Step 4: A complete training process consists of a forward propagation and a backward propagation. In order to realize the network back propagation process, the Adaptive moment estimation (Adam)[20] of deep learning adaptive learning rate optimization algorithm is used. The weights and biases of the network are updated according to the gradient of the loss function. Adam is defined by the following composite function;

$$u_t = \beta_1 u_{t-1} + (1-\beta_1) f_t\ (\theta_t) \tag{6}$$

ISSN: 2472-3703 DOI: 10.6911/WSRJ.202502_11(2).0002

$$o_t = \beta_2 o_{t-1} + (1-\beta_2) f_t^2(\theta_t) \tag{7}$$

$$\hat{u}_t = u_t / (1-\beta_1^t) \tag{8}$$

$$\hat{o}_t = o_t / (1-\beta_2^t) \tag{9}$$

$$\theta_{t+1} = \theta_t - \alpha \hat{u}_t / (\sqrt{\hat{o}_t} + \varepsilon) \tag{10}$$

f_t and f_t^2 represent the first and second derivatives of the objective function with respect to parameters when the time step is t; m_t and v_t represent the first and second moment estimation of the gradient respectively, which is the approximate representation of the expected $E[f_t(\theta_t)]$, $E[f_t^2(\theta_t)]$. β_1 and β_2 respectively represent the attenuation rates estimated by the first-order and second-order moments; α stands for learning rate; ε is the constant term; $\hat{u}_t$ and $\hat{o}_t$ represent the correction of u_t and o_t, which are approximately unbiased estimates of expectations. Adam algorithm dynamically adjusts the learning rate of each parameter by using the first and second order moment estimation of the gradient.

When constructing the FCDNN model, the default parameter Settings of Adam algorithm in TensorFlow deep learning framework are used, this is $\alpha = 0.001$, $\beta_1 = 0.9$, $\beta_2 = 0.999$, $\varepsilon = 10^{-8}$. After the parameters α, β_1, β_2 and the random objective function $f(\theta)$ are determined, the parameter vector, the first-order moment vector, the second-order moment vector and the time step are initialized. When parameter θ does not converge, each part is iteratively updated. The specific operation is: time step t add l; Update the gradient of the objective function to the parameter θ on the time step; First order moment estimation and second order original moment estimation of updating loss; The first-order and second-order moment estimators of loss correction are calculated. Update the model parameter θ by iterating the values obtained by the above calculation steps.

3. DATA ACQUISITION AND DATA PREPROCESSING

3.1. Data acquisition

All the data came from the CALCE battery research group at the university of Maryland. CALCE battery research group is committed to developing the latest BMS for single-battery and multi-battery systems to provide the most accurate SOH indicators for SOC and health status.

The data set of K2 lithium iron phosphate battery in CALCE was used. Download the dataset numbered K2-016. The data set used in the experiment included 4390 samples and 27 charge and discharge cycles. The training set consists of 4227 samples, including 26 charge and discharge cycles. The test set consists of 163 samples, including 1 charge and discharge cycle.

The partial charge-discharge data of training set and verification set are shown in table 1. The resistance, current, voltage and SoC values are the real data of K2 lithium iron phosphate battery.

ISSN: 2472-3703 DOI: 10.6911/WSRJ.202502_11(2).0002

Table 1. Partial charge-discharge data

Resistance/Ω	Current/A	Voltage/V	SOC real value/%
0.040821668	0	2.635535955	0
0.040821668	2.599924326	2.98563695	1.412
0.040821668	2.599744081	3.080854177	2.824
0.040821668	2.600104809	3.146761417	4.237
0.039621029	0	3.799679041	100
0.039621029	-2.599911213	3.213963985	98.587
0.039621029	-2.599550724	3.196313143	97.174
0.039621029	-2.599730968	3.189188004	95.761571

The variation trend of current and voltage of the training set data is shown in Fig.3(left). The variation trend of current and voltage of test set data is shown in Fig.3(right).

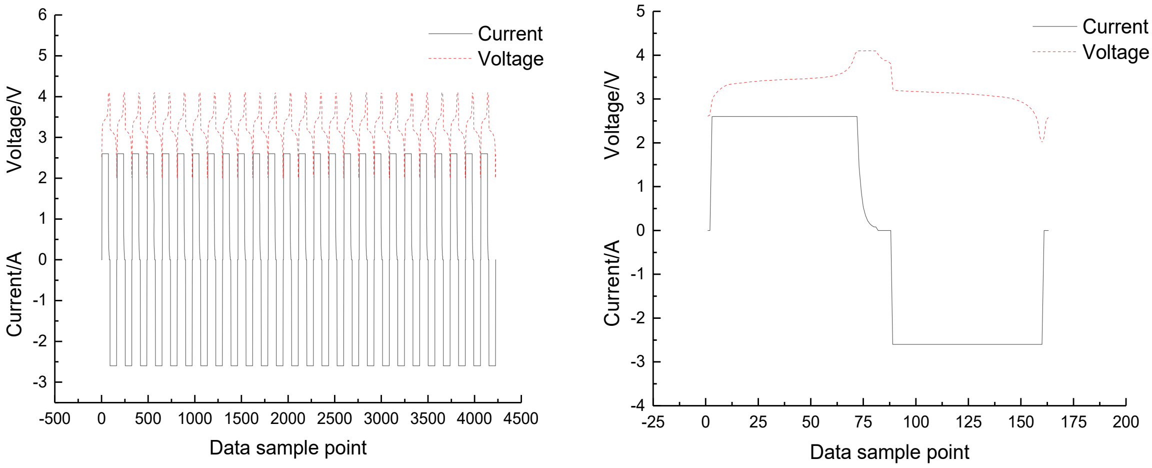

Figure 3. Voltage and current of the training set (left) and the test set (right)

The change curve of the relationship between voltage and SoC during charging and discharging is shown in Fig.4(left). The real SoC value change curve of the whole training set is shown in Fig.4(right).

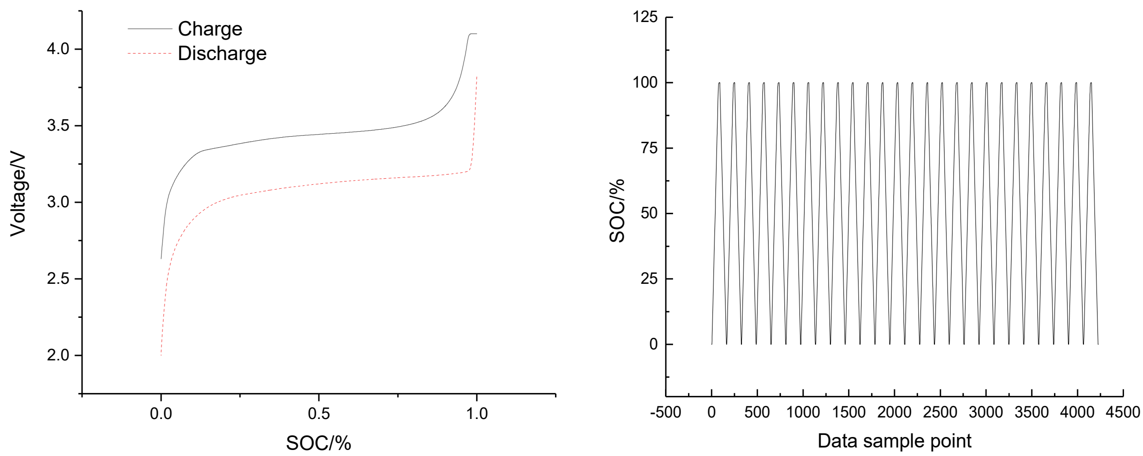

Figure 4. Charge-discharge voltage and SoC relationship curve (left), and training set SoC real value (right)

ISSN: 2472-3703 DOI: 10.6911/WSRJ.202502_11(2).0002

3.2. Data preprocessing

The 4-fold cross validation method divides the data of the training set into 4 partitions of the same size. Then the data of three partitions were selected to train the model, and the fourth partition was reserved to verify the model. This process is repeated four times, each time using a different reserved partition to validate the model[21]. In other words, the model was trained and validated four times per iteration. Get MSE and MAE after 4 validations. The mean values of MSE and MAE were obtained.

The principle and structure of the 4-fold cross validation method are shown in Fig.5;

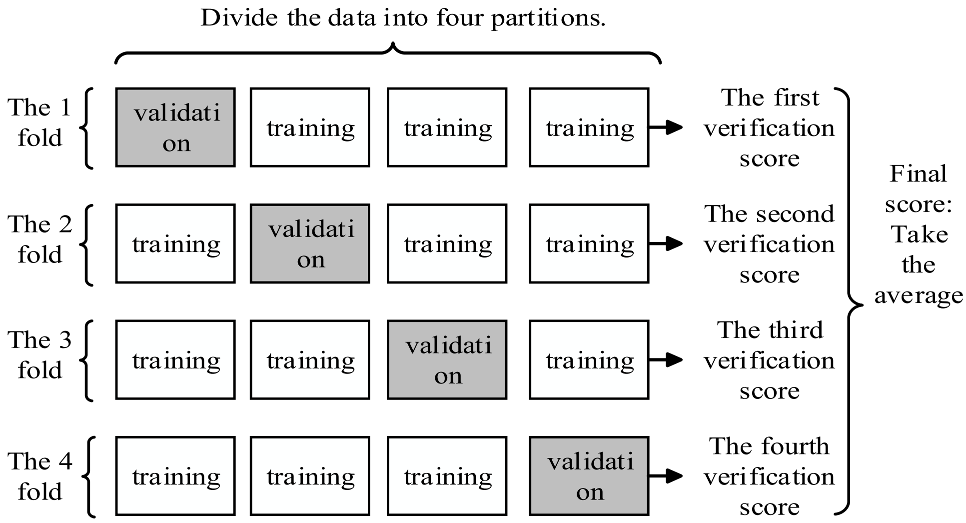

Figure 5. The principle and structure of the 4-fold cross validation method

Due to the different value ranges of various data in the data set, it is necessary to normalize the resistance, current and voltage of the original data. If the data with different value ranges are used in the model training process, the model will automatically adapt to the data with different value ranges, but the learning process of the model will become difficult. The data normalization formula is shown below;

$$x' = \frac{x - \mu}{\sigma} \tag{11}$$

In the formula: μ is the mean, σ is the standard deviation. The normalization process makes all the data gather around 0 and the variance is 1.

4. ANALYSIS OF EXPERIMENTAL RESULTS

During the training and validating the model, the FCDNN outputs the MAE value of 800 training epochs to monitor the training status of the model. By observing the change trend of MAE value, the optimal iteration steps of the model were determined. Save the trained model for use by the test set.

The FCDNN model was constructed with Fully Connected Layers (FCL). Fig.6 shows the training framework of SoC prediction model for lithium batteries based on FCDNN model.

ISSN: 2472-3703 DOI: 10.6911/WSRJ.202502_11(2).0002

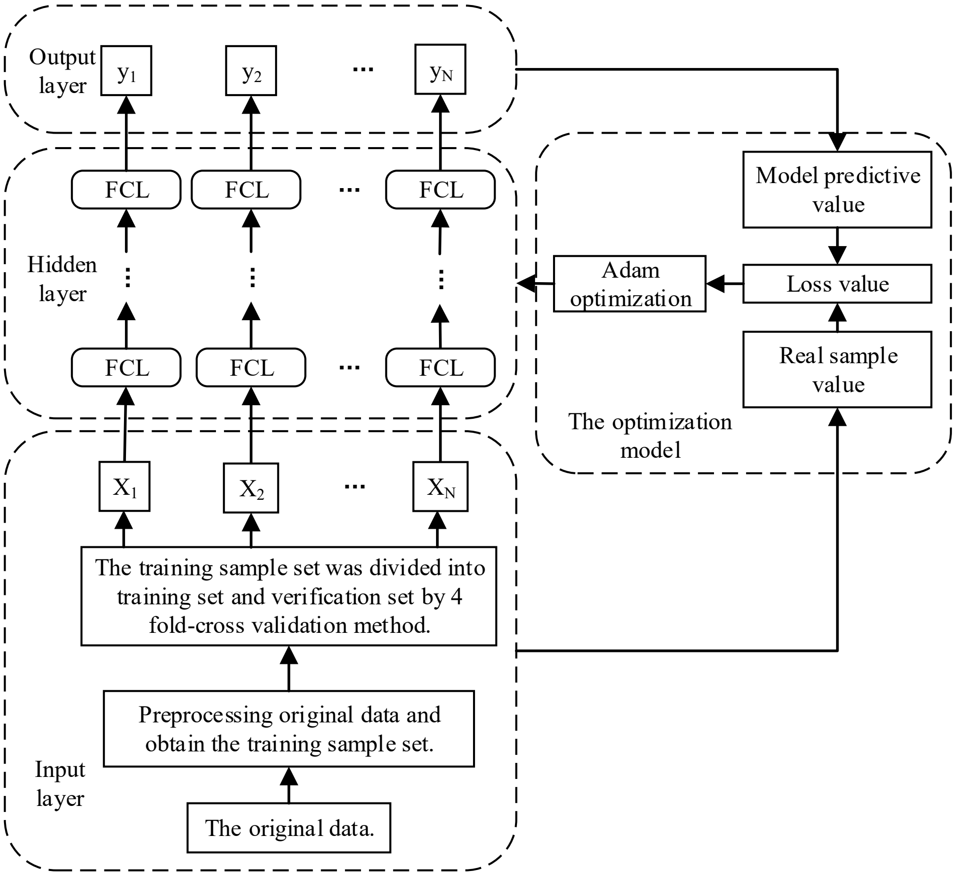

Figure 6. SoC prediction model training framework of lithium battery based on FCDNN model

Fig.7(left) shows the MAE value change curve during the training of 4-layer FCDNN model. Fig.7(right) shows the MAE change curve with the first 10 iteration rounds removed. The 4-layer FCDNN model iterates through 688 epochs to obtain the optimal weight parameters. The MAE value of this model was 1.2250387958290936%. The estimated time for a single sample is 2ms. Fig.8 is the curve diagram of the SoC estimated value of the model and the real value of SoC.

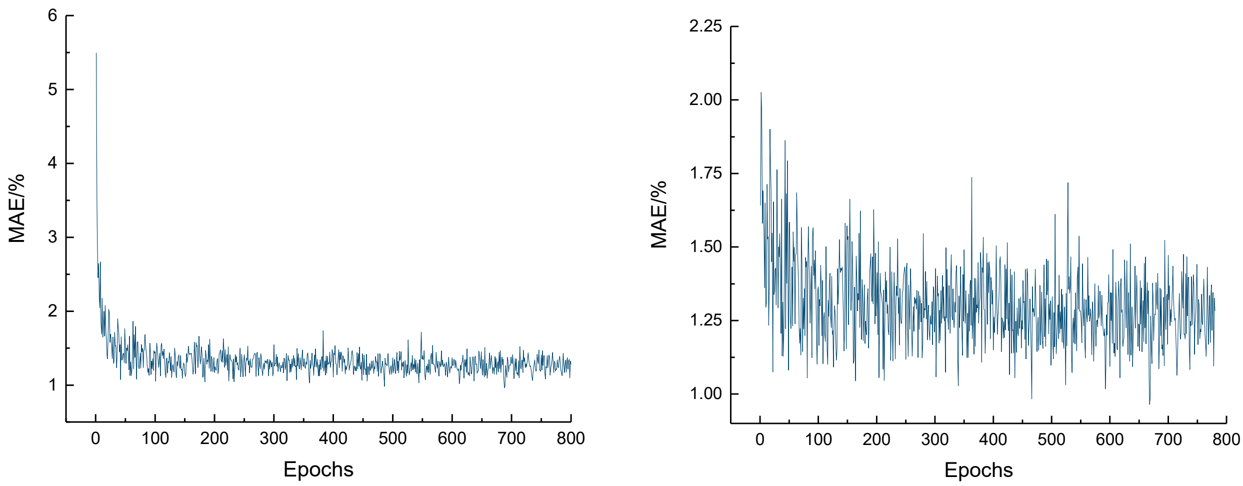

Figure 7. MAE change curve of the 4-layer FCDNN model (left) and after removing the first 10 epochs (right)

ISSN: 2472-3703 DOI: 10.6911/WSRJ.202502_11(2).0002

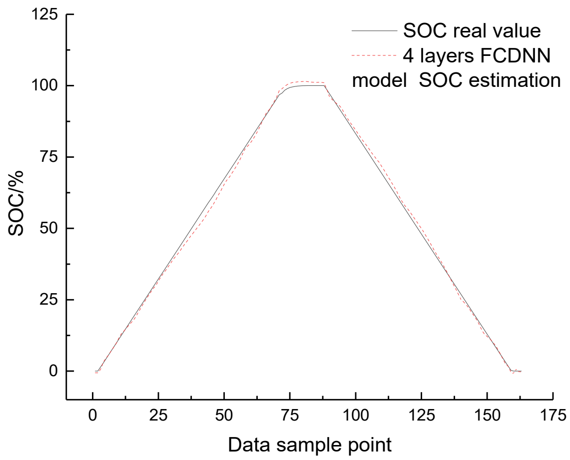

Figure 8. SoC estimate and real value comparison curve the 4-layer FCDNN model

Fig.9(left) shows the MAE value change curve during the training of the 8-layer FCDNN model. Fig.9(right) shows the MAE change curve with the first 10 iteration rounds removed. The 8-layer FCDNN model iterates through 50 epochs to obtain the optimal weight parameters. The MAE value of the model was 0.9541996553300257%. The estimated time for a single sample is 5ms. Fig.10 is the curve diagram of the SoC estimated value of the model and the true value of SoC.

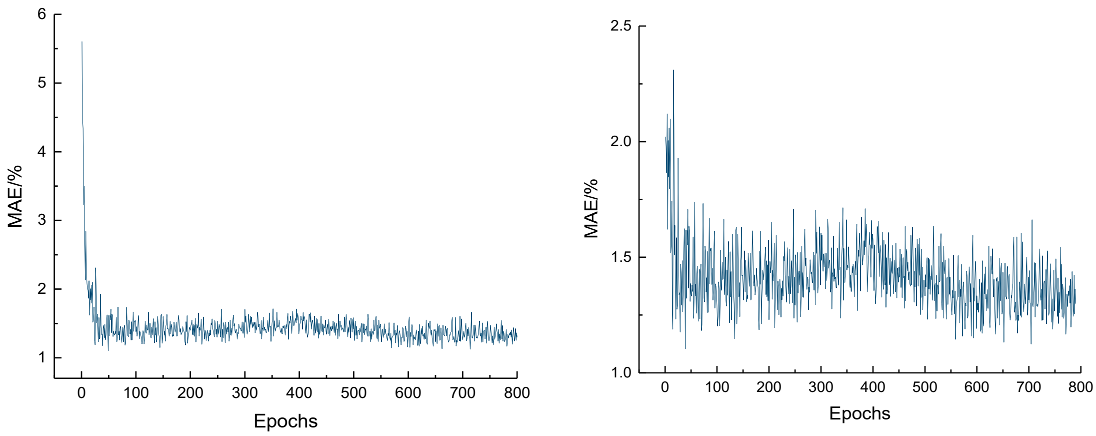

Figure 9. MAE change curve of the 8-layer FCDNN model (left) and after removing the first 10 epochs (right)

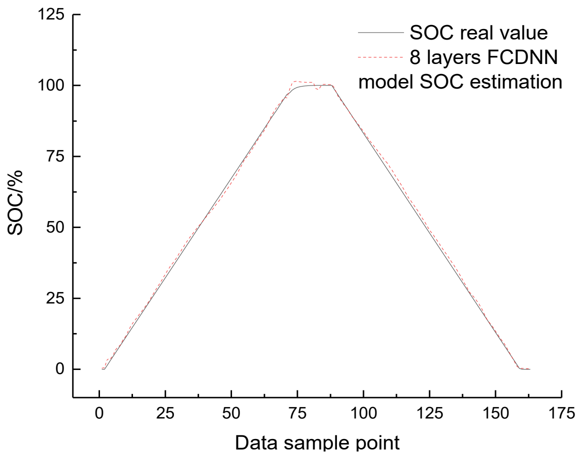

Figure 10. SoC estimate and real value comparison curve of the 8-layer FCDNN model

ISSN: 2472-3703 DOI: 10.6911/WSRJ.202502_11(2).0002

Fig.11(left) shows the MAE value change curve during the 12-layer FCDNN model training. Fig.11(right) shows the MAE change curve with the first 10 iteration rounds removed. The 12-layer FCDNN model iterates through 553 epochs to obtain the optimal weight parameters. The MAE value of this model is 1.3063968141760357%. The estimated time for a single sample is 5ms. Fig.12 is the curve diagram of the SOC estimated value of the model and the true value of SOC.

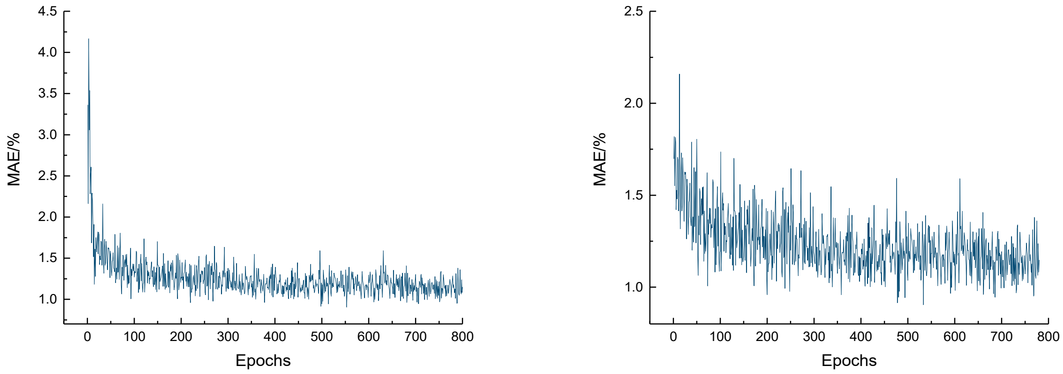

Figure 11. MAE change curve of the 12-layer FCDNN model (left) and after removing the first 10 epochs (right)

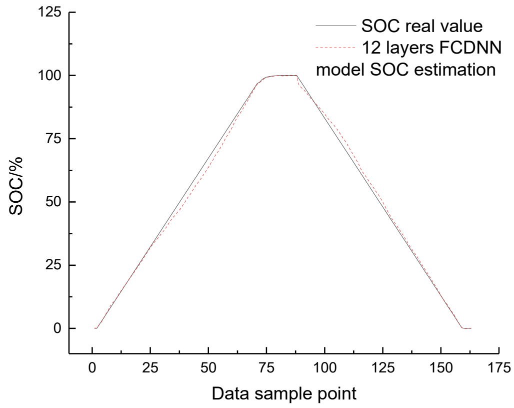

Figure 12. SoC estimate and real value comparison curve of the 12-layer FCDNN model

The SoC estimation errors of FCDNN models at layers 4, 8 and 12 are shown in fig.13(left). The estimation error of the 4-layer FCDNN model is kept within 3.5%. The error graph of the 8-layer FCDNN model has a smaller fluctuation range and the estimated error is kept within 3%. The estimation error of the 12-layer FCDNN model is kept within 4%. It can be seen that the deeper FCDNN model can no longer estimate the SoC value more accurately. According to the data set used in the experiment, the 8-layer FCDNN model can accurately predict the SoC of lithium battery in a suitable range.

Fig.13(right) shows the error comparison curve between the estimated SOC value and the real SOC value of the 8-layer FCDNN model, BPNN model and ampere-hour integral method. The test data set includes data for the 27th charge-discharge cycle. In the process of 27 charge-discharge cycles, the SOC estimation error of ampere-hour integration method has reached between 8% and 10%, and the errors will be accumulated continuously with the increase of

ISSN: 2472-3703 DOI: 10.6911/WSRJ.202502_11(2).0002

charge-discharge cycles. The estimation error of the traditional BPNN model is kept within 5%, while that of the 8-layer FCDNN model is kept at 3%.

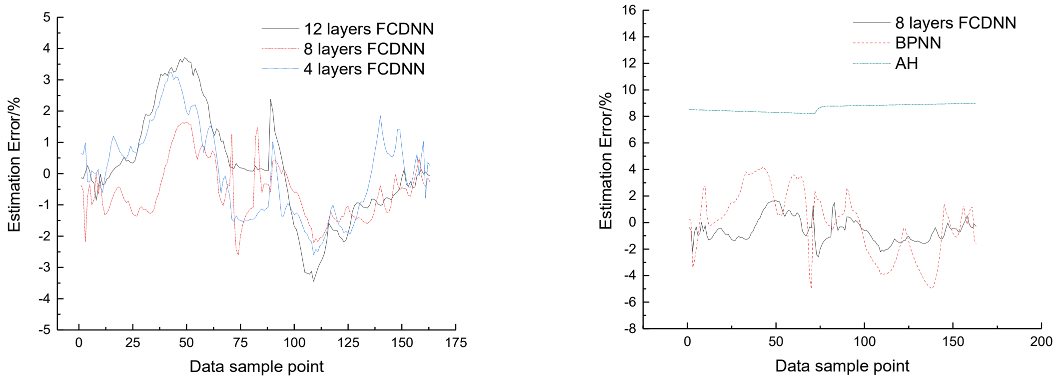

Figure 13. Comparison of SoC estimation error values: (left) FCDNN models with 4, 8, and 12 layers, (right) the 8-layer FCDNN model, BPNN model, and ampere-hour integration method

Input the test set data into the trained 8-layer FCDNN model. Part of the data of SoC estimate value and estimated error value of the model are shown in table 2.

Table 2. Partial estimation results of the 8-layer FCDNN model

Resistance/Ω	Current/A	Voltage/V	SoC real value/%	SoC estimate value/%	Error value/%
0.027214	0	2.63084	0	0.547532	-0.548
0.027214	2.599744	2.977055	1.4032	3.590534	-2.187
0.027214	2.599744	3.138665	4.209594	4.535218	-0.326
0.027214	2.599924	3.189512	5.61282	6.610165	-0.997
0.050596	0	3.819273	1	100.3371	-0.337
0.050596	-2.59955	3.219955	98.595281	99.18515	-0.59

5. CONCLUSION

The SoC estimation of lithium battery is the key technology of BMS. The data set of K2 lithium iron phosphate battery measured by CALCE battery research group, university of Maryland, USA was used. Aiming at the deficiency of mapping degree of shallow neural network algorithm; The SoC of lithium iron phosphate battery was estimated by FCDNN model.

(1) The FCDNN model can be trained by 4-fold cross validation to make full use of the data set. Get accurate verification MAE; Thus, the best epochs for the training model are determined.

(2) Relu activation function prevents FCDNN model from disappearing as the network depth increases. Adam, an adaptive learning rate optimization algorithm in TensorFlow deep learning framework, is used to replace the traditional gradient descent algorithm to update FCDNN model parameters.

(3) Based on the Juypter Notebook platform and supported by TensorFlow and Keras, FCDNN simulation models with three depths were established, and the SoC estimation errors were compared with the ampere-hour integration method and the traditional BPNN model. Experiments verify that the SoC estimation error of the 8-layer FCDNN model with 10 nodes at

each hidden layer is kept within 3%. The MAE is 0.9541996553300257%. The estimated time for a single sample is 5ms. The estimation effect of the FCDNN model is better than the traditional BPNN and the ampere-hour integration method.

ACKNOWLEDGMENTS

This paper is supported by the Key Research and Development Program in Henan Province (231111210500) and the National Key R&D Program of China: Key technical equipment for disaster monitoring, warning, and information acquisition based on communication big data (2023YFC3010700).

REFERENCES

[1] Xu J, Cai X, Cai S, et al. High-energy lithium-ion batteries: recent progress and a promising future in applications[J]. Energy & Environmental Materials, 2023, 6(5): e12450.

[2] Urquizo J, Singh P. A review of health estimation methods for Lithium-ion batteries in Electric Vehicles and their relevance for Battery Energy Storage Systems[J]. Journal of Energy Storage, 2023, 73: 109194.

[3] Fang Y, Zhang Q, Zhang H, et al. State-of-charge estimation technique for lithium-ion batteries by means of second-order extended Kalman filter and equivalent circuit model: Great temperature robustness state-of-charge estimation[J]. IET Power Electronics, 2021, 14(8): 1515-1528.

[4] Hannan M A , Lipu M S H , Hussain A , et al. Neural Network Approach for Estimating State of Charge of Lithium-ion Battery Using Backtracking Search Algorithm[J]. IEEE Access, 2018, 6(2018):10069-10079.

[5] Zhang X, Hou J, Wang Z, et al. Study of SOC estimation by the ampere-hour integral method with capacity correction based on LSTM[J]. Batteries, 2022, 8(10): 170.

[6] Ren Z, Du C, Wu Z, et al. A comparative study of the influence of different open circuit voltage tests on model-based state of charge estimation for lithium-ion batteries[J]. International journal of energy research, 2021, 45(9): 13692-13711.

[7] Ephrem Chemali, Phillip J. Kollmeyer, Matthias Preindl, et al. State-of-charge estimation of Li-ion batteries using deep neural networks: A machine learning approach[J]. Journal of Power Sources, 2018,400.

[8] Kaniewski P. Extended Kalman filter with reduced computational demands for systems with non-linear measurement models[J]. Sensors, 2020, 20(6): 1584.

[9] Kaviani S, Sohn I. Application of complex systems topologies in artificial neural networks optimization: An overview[J]. Expert Systems with Applications, 2021, 180: 115073.

[10] Lipu M S H , Hannan M A , Hussain A , et al. State of Charge Estimation for Lithium-ion Battery Using Recurrent NARX Neural Network Model Based Lighting Search Algorithm[J]. IEEE Access, 2018, 6(2018):28150-28161.

[11] Cai B, Li M, Yang H, et al. State of Charge Estimation of Lithium-Ion Battery Based on Back Propagation Neural Network and AdaBoost Algorithm[J]. Energies, 2023, 16(23): 7824.

[12] Zhang Z, Chen S, Lu L, et al. High-Precision and Robust SOC Estimation of LiFePO4 Blade Batteries Based on the BPNN-EKF Algorithm[J]. Batteries, 2023, 9(6): 333.

[13] Tao S, Jiang B, Wei X, et al. A systematic and comparative study of distinct recurrent neural networks for lithium-ion battery state-of-charge estimation in electric vehicles[J]. Energies, 2023, 16(4): 2008.

ISSN: 2472-3703 DOI: 10.6911/WSRJ.202502_11(2).0002

[14] Yahia A, Tamer M, Shahin M, et al. Advances in Lithium-Ion Battery SOC Prediction: A Data-Driven GRU-RNN Framework[C]//2023 11th International Japan-Africa Conference on Electronics, Communications, and Computations (JAC-ECC). IEEE, 2023: 253-258.

[15] Nishanthy J, Sivakumar N. Deep Learning based EV Battery Management System[C]//2023 International Conference on Energy, Materials and Communication Engineering (ICEMCE). IEEE, 2023: 1-5.

[16] Pattanayak S. Introduction to deep-learning concepts and TensorFlow[M]//Pro Deep Learning with TensorFlow 2.0: A Mathematical Approach to Advanced Artificial Intelligence in Python. Berkeley, CA: Apress, 2023: 109-197.

[17] CALCE. Lithium-Ion Battery Experimental Data. Accessed: Jan. 5, 2017.[Online]. Available: http://www.calce.umd.edu/batteries/data.htm.

[18] Wang P, Fan E, Wang P. Comparative analysis of image classification algorithms based on traditional machine learning and deep learning[J]. Pattern recognition letters, 2021, 141: 61-67.

[19] Karypidis E, Mouslech S G, Skoulariki K, et al. Comparison Analysis of Traditional Machine Learning and Deep Learning Techniques for Data and Image Classification [J]. arXiv preprint arXiv:2204.05983, 2022.

[20] D.P. Kingma and J. Ba. Adam: a method for stochastic optimization, CoRR abs/1412.6980, http://arxiv.org/abs/1412.6980.

[21] Wieczorek J, Guerin C, McMahon T. K-fold cross-validation for complex sample surveys[J]. Stat, 2022, 11(1): e454.